# Supporting Information:

## Solvent-controlled 3D Lanthanide-Polyoxometalate Frameworks: Reduction and Stabilization of Ag Nanocomposites and Catalytic Properties

**Guang-Gang Gao,[a,c] Chao-Yu Song,[a] Xi-Ming Zong,[a] Dong-Feng Chai,[a] Hong Liu*[a], Yu-Long Zou,[a] Jian-Xun Liu,[a] and Yun-Feng Qiu*[b]**

[a] College of Pharmacy, Jiamusi University, Jiamusi 154004, China.

[b] State Key Lab of Urban Water Resource and Environment (SKLUWRE) & Academy of Fundamental and Interdisciplinary Science, Harbin Institute of Technology, Harbin, Heilongjiang, 150080, P.R. China

[c] Department of Chemistry, Changchun Normal University, Changchun 130032, China.

*Corresponding authors: liuhong_chem@163.com; qiuyf@hit.edu.cn

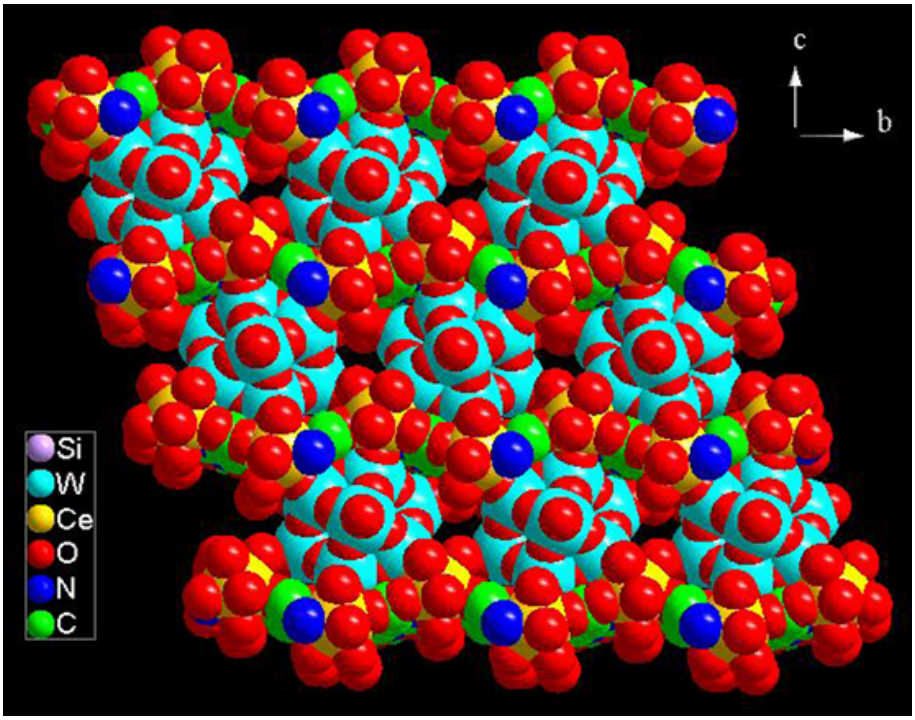


**Fig. S1** Space-filling view of 3D architecture of **4** along *a* axes.

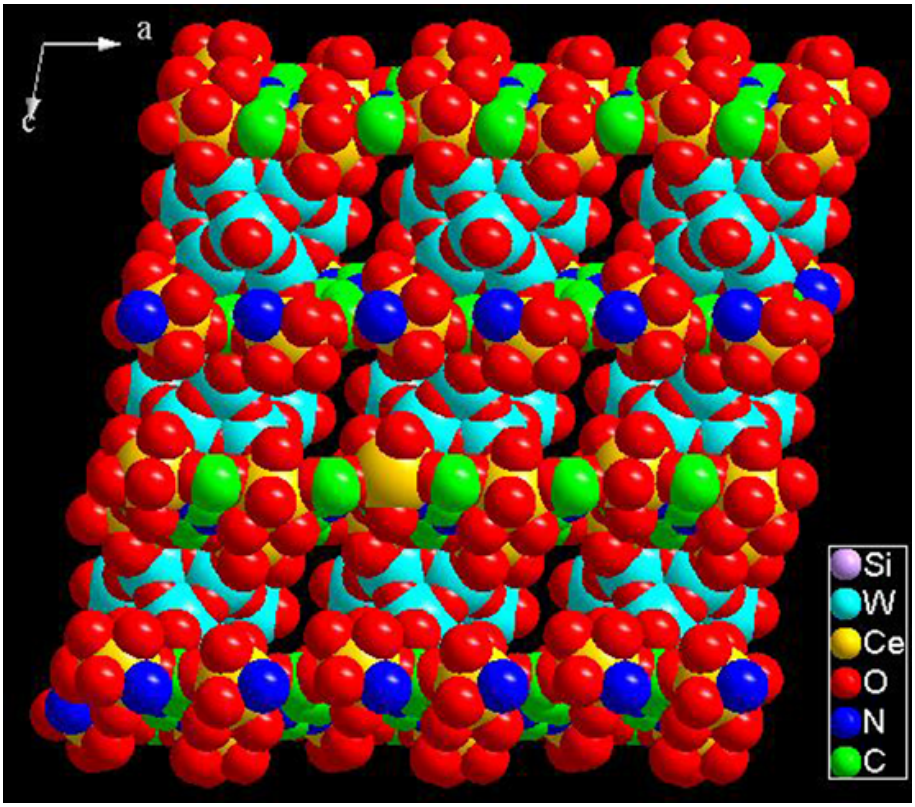


**Fig. S2** Space-filling view of 3D architecture of **4** along *b* axes.

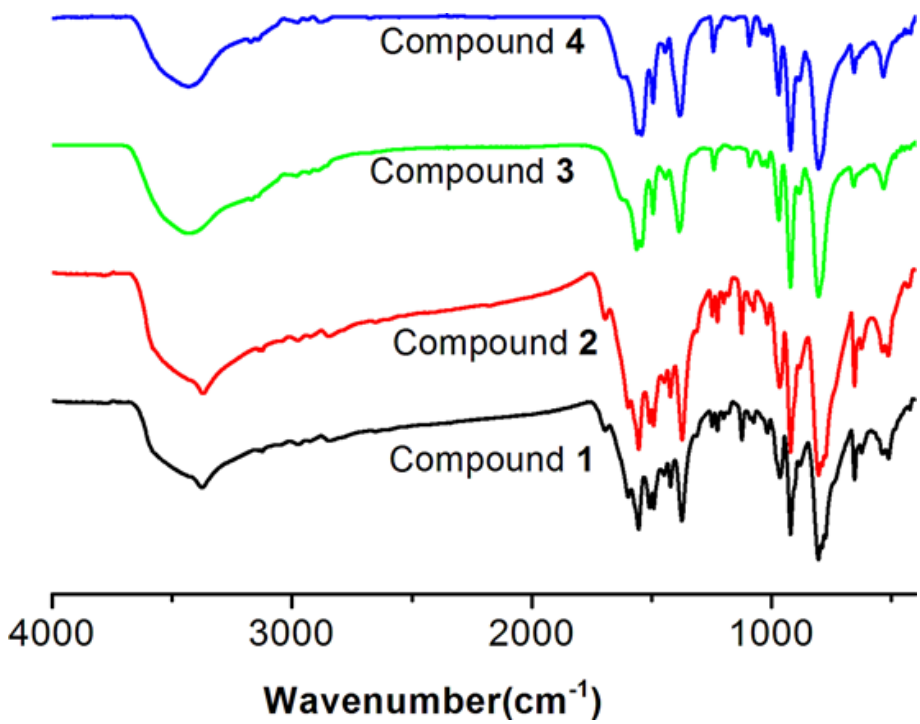


**Fig. S3** FT-IR of compounds **1** to **4**.

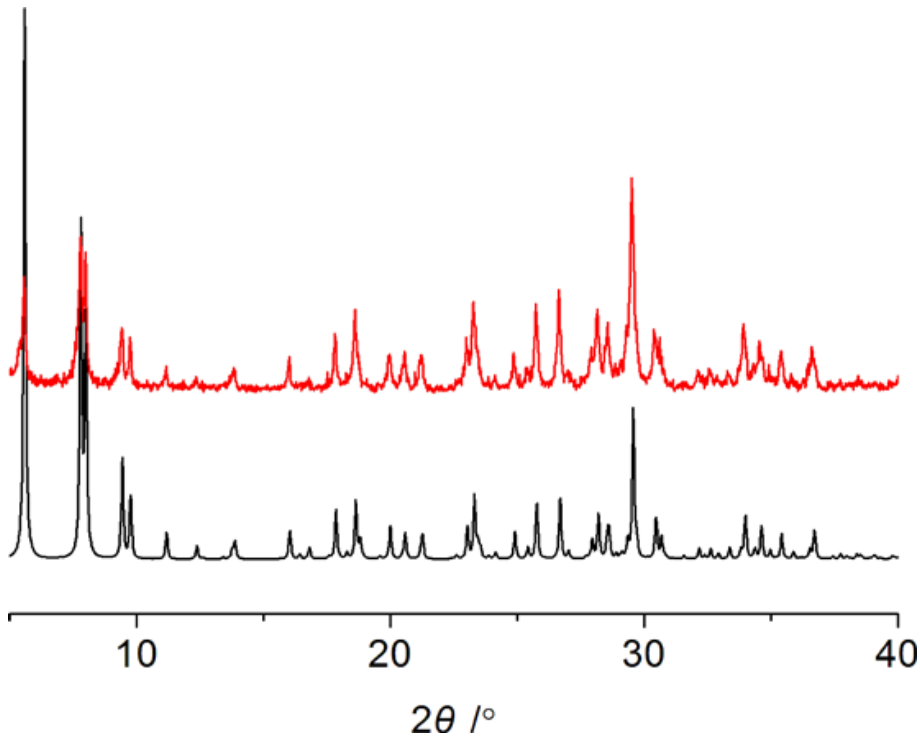


**Fig. S4** Experimental powder X-ray diffraction (PXRD) pattern of **1** (red) and simulated PXRD pattern of **1** (black).

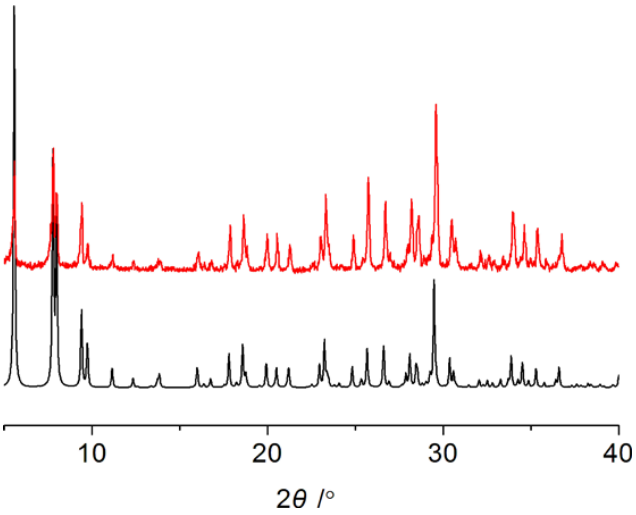


**Fig. S5** Experimental powder X-ray diffraction (PXRD) pattern of **2** (red) and simulated PXRD pattern of **2** (black).

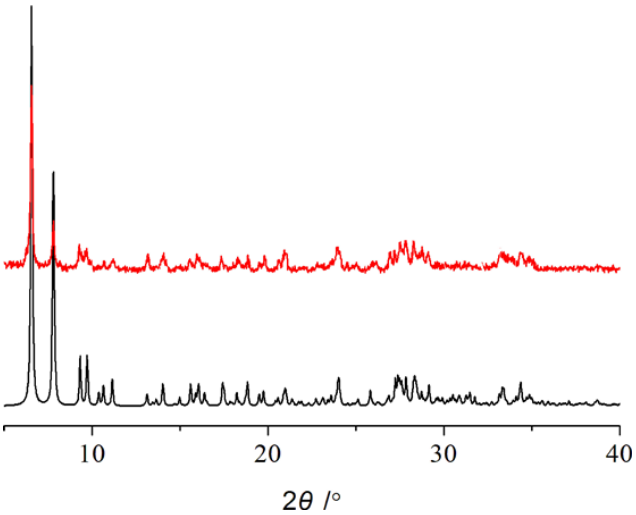


**Fig. S6** Experimental powder X-ray diffraction (PXRD) pattern of **3** (red) and simulated PXRD pattern of **3** (black).

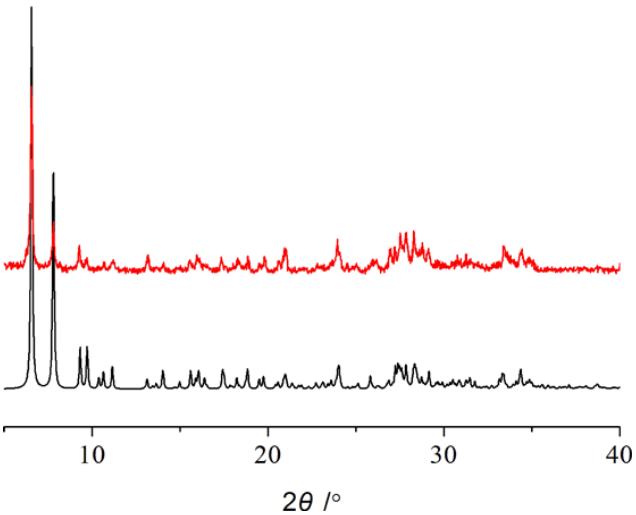


**Fig. S7** Experimental powder X-ray diffraction (PXRD) pattern of **4** (red) and simulated PXRD pattern of **4** (black).

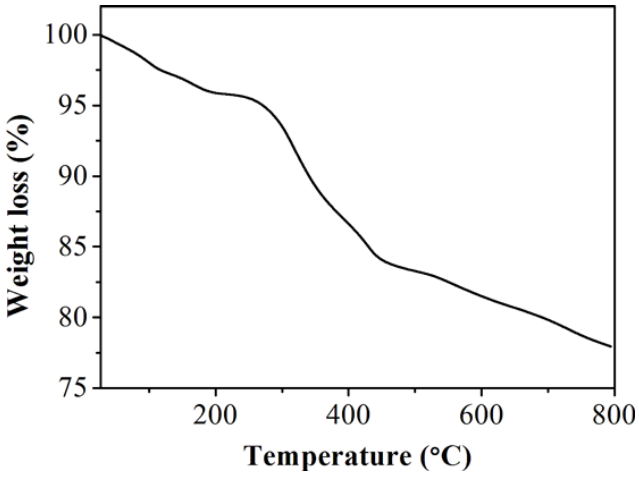


**Fig. S8** TG curve of compound **1**.

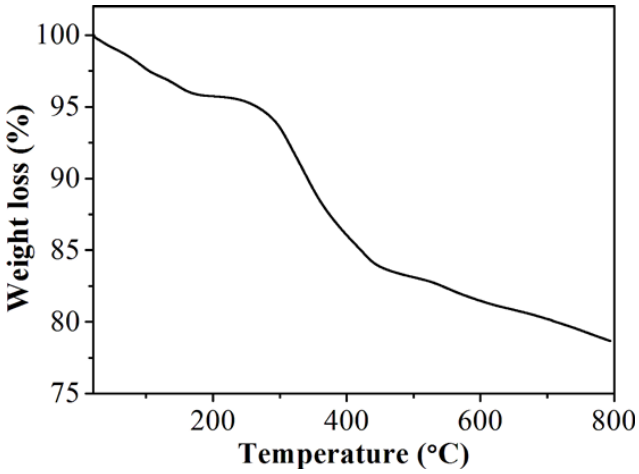


**Fig. S9** TG curve of compound **2**.

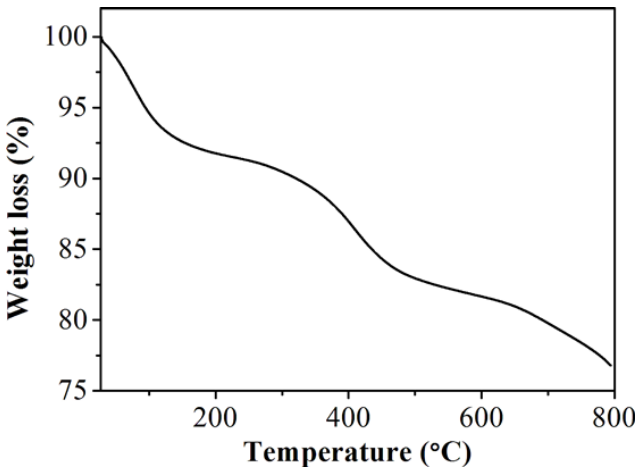


**Fig. S10** TG curve of compound **3**.

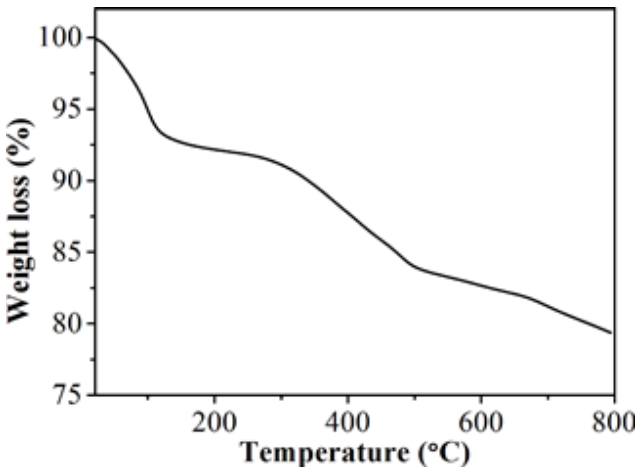


**Fig. S11** TG curve of compound **4**.

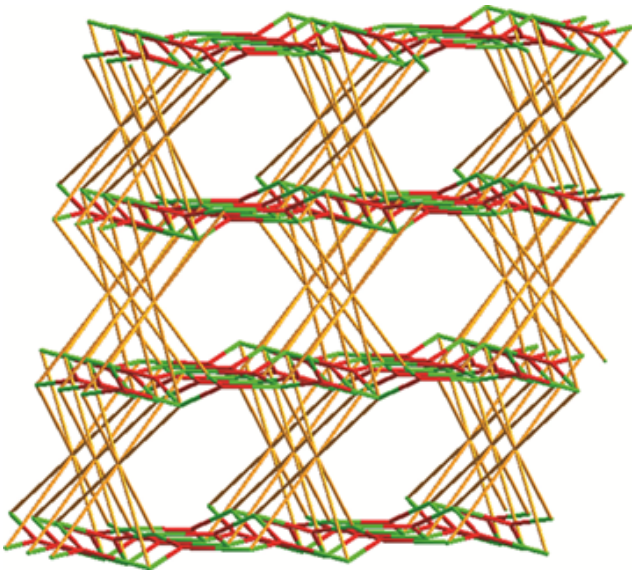

**Fig. S12** View of the topology of compound **3** or **4** (yellow nodes represent polyoxoanions; green nodes represent Ln ions; red nodes represent $H_3IDC$ ligand).

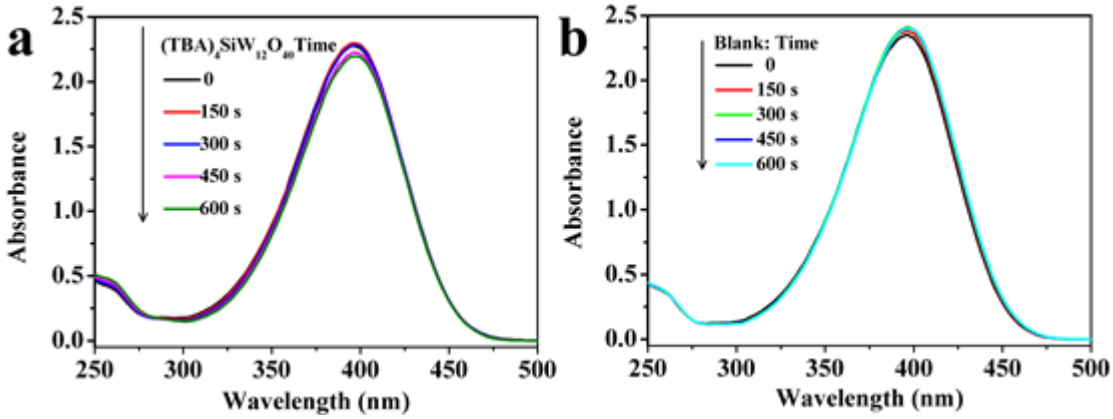


**Fig. S13** (a) and (b) are absorption spectra of 4-nitrophenolate ion in distilled water during the reduction reaction in the presence of $NaBH_4$ with the catalysts of Ag@$(TBA)_4SiW_{12}O_{40}$ and without catalyst, respectively. The characteristic peak intensity of 4-nitrophenolate ion was unchanged. The results illustrated that $(TBA)_4SiW_{12}O_{40}$ as solid salts without any porous structural features was not ideal supports for the loading of Ag, and thus showed poor catalytic activity towards the reduction of 4-NP. Additionally, the reduction reaction couldn't proceed efficiently only in the presence of $NaBH_4$ itself without any catalysts.

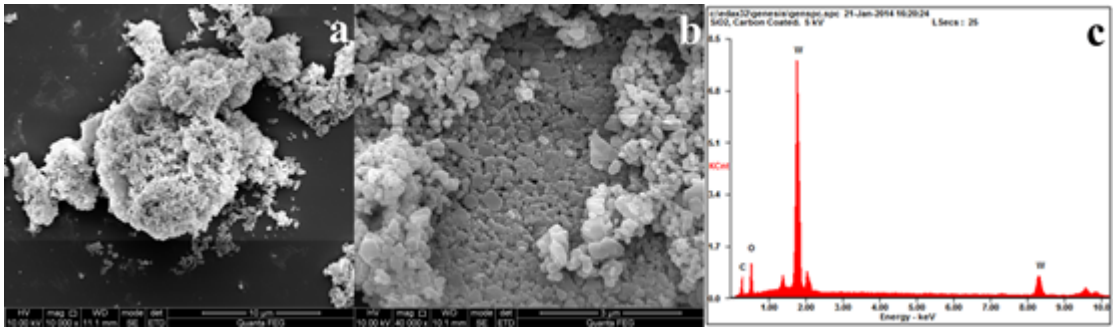


**Figure S14**. (a) and (b) are SEM images of $(TBA)_4SiW_{12}O_{40}$ powder before and after loading Ag nanostructures. (c) is the corresponding EDS of Ag@$(TBA)_4SiW_{12}O_{40}$ composites. However, Ag loading amount on the surface of $(TBA)_4SiW_{12}O_{40}$ is quite low due to the poor affinity of Ag ions and the hydrophobic surface of $(TBA)_4SiW_{12}O_{40}$ powders. Thus, the Ag loading amount might be too low to detect under EDS due to the detection limit. The preparation procedure of Ag@$(TBA)_4SiW_{12}O_{40}$ was similar with that of Ag@Crystals.

Table.S1 Selected bond lengths (Å) associated with the La coordination environments in **1**.

| | |
|---|---|
| La-O(17)#3 | 2.458(9) |
| La-O(16)#3 | 2.481(8) |
| La-O(15) | 2.496(8) |
| La-O(19) | 2.526(9) |
| La-O(6)#3 | 2.589(7) |

Table.S2 Selected bond lengths (Å) associated with the Ce coordination environments in **2**.

| | |
|---|---|
| Ce-O(17)#3 | 2.461(5) |
| Ce-O(16)#3 | 2.482(5) |
| Ce-O(15) | 2.499(4) |
| Ce-O(19) | 2.534(5) |
| Ce-O(6)#3 | 2.604(4) |
| Ce-O(23) | 2.616(5) |
| Ce-O(8) | 2.650(4) |
| Ce-N(1) | 2.679(5) |
| Ce-N(3) | 2.790(6) |

Table.S3 Selected bond lengths (Å) associated with the Ce coordination environments in **3**.

| | | | |
|---|---|---|---|
| La(2)-O(24) | 2.42(2) | La(1)-O(32)#4 | 2.450(19) |
| La(2)-O(26) | 2.447(18) | La(1)-O(30)#4 | 2.476(18) |
| La(2)-O(31)#2 | 2.48(2) | La(1)-O(23) | 2.522(18) |
| La(2)-O(29) | 2.501(18) | La(1)-O(20) | 2.52(2) |
| La(2)-O(27) | 2.57(2) | La(1)-O(25)#3 | 2.55(2) |
| La(2)-N(3) | 2.61(2) | La(1)-O(22) | 2.57(3) |
| La(2)-O(28) | 2.61(2) | La(1)-O(15)#5 | 2.61(3) |
| La(2)-O(8)#3 | 2.71(2) | La(1)-N(2)#3 | 2.65(2) |
| La(2)-O(17)#1 | 2.84(2) | La(1)-O(21) | 2.73(4) |

Table.S4 Selected bond lengths (Å) associated with the Ce coordination environments in **4**.

| | | | |
|---|---|---|---|
| Ce(2)-O(25) | 2.478(13) | Ce(1)-O(32)#4 | 2.416(13) |
| Ce(2)-O(20) | 2.491(14) | Ce(1)-O(30)#4 | 2.430(13) |
| Ce(2)-O(24) | 2.499(13) | Ce(1)-O(23) | 2.459(14) |
| Ce(2)-O(31)#2 | 2.522(13) | Ce(1)-O(26)#5 | 2.506(14) |
| Ce(2)-O(29) | 2.536(14) | Ce(1)-O(22) | 2.544(17) |
| Ce(2)-O(3)#3 | 2.541(15) | Ce(1)-O(21) | 2.542(16) |
| Ce(2)-O(28) | 2.58(3) | Ce(1)-N(1) | 2.595(17) |
| Ce(2)-O(27) | 2.60(2) | Ce(1)-O(19) | 2.671(16) |
| Ce(2)-N(4) | 2.660(17) | Ce(1)-O(14)#2 | 2.805(15) |